



ORIGINAL ARTICLE

Reconstruction of the cervical spinal cord based on motor function restoration and mitigation of oxidative stress and inflammation through eNOS/Nrf2 signaling pathway using ibuprofen-loaded nanomicelles



Yang Yang^a, Lei Zhang^b, Meiyi Huang^c, Rubo Sui^{c,*}, Suliman Khan^{d,*}

^a Jinzhou Medical University, Jinzhou 121001, China

^b School of Nursing, Jinzhou Medical University, Jinzhou 121001, China

^c Department of Neurology, the First Affiliated Hospital of Jinzhou Medical University, Jinzhou 121001, China

^d Department of Cerebrovascular Diseases, The Second Affiliated Hospital of Zhengzhou University, Zhengzhou, China

Received 19 April 2021; accepted 20 June 2021

Available online 25 June 2021

KEYWORDS

Spinal cord injury;
Cervical;
Reconstruction;
Nanomicelle;
Ibuprofen;
Electrophysiology;
Inflammation;
Oxidative stress;
Signaling pathway

Abstract Motor dysfunction and oxidative and inflammatory stress after spinal cord injuries (SCIs) occur as a result of primary mechanical damage and secondary degeneration process. In the present study, we aimed to examine the protective effect of fabricated ibuprofen- polyethylene glycol (PEG)/polylactide acid (PLA) diblock copolymer nanomicelles on reconstruction of motor-evoked potential (MEP) of cervical spinal cord, the posterior limb function, ROS and RNS levels, expression of inflammation cytokines, and enzymatic and non-enzymatic antioxidant systems after an experimental SCI. Also, qPCR assay was employed to assess eNOS and Nrf2 at the mRNA level. It was shown that that the drug loading and entrapment efficiency of fabricated nanomicelles were around 9.3% and 72.09%, respectively. Also, the average size and zeta potential of blank PEG-PLA diblock copolymer nanomicelles and drug-loaded nanomicelles were 32.4 ± 2.18 nm, 36.2 ± 2.0 nm and -21.73 ± 4.21 mV, -34.48 ± 3.38 mV, respectively. Moreover, ibuprofen-PEG/PLA diblock copolymer nanomicelles revealed a slight burst release within the first 20 h, followed by a continuous release phase over 12 h. It was seen that in control group, MEP amplitude decreased to 17.41 ± 3.75 mV at 1 h after surgery, whereas MEP amplitudes in ibuprofen- and ibuprofen-PEG/PLA -nanomicelles- treated animals were remarkably increased in comparison with the con-

* Corresponding authors.

E-mail addresses: rsui.jmu@yahoo.com (R. Sui), suliman.khan18@mails.ucas.ac.cn (S. Khan).

Peer review under responsibility of King Saud University.



Production and hosting by Elsevier

trol group, and this enhancement was more pronounced for ibuprofen-PEG/PLA -treated animals. Finally, it was determined that compared with those in the SCI group, the spinal cord function score, SOD, CAT and GSH levels in the ibuprofen-PEG/PLA -nanomicelles- treated group were significantly increased, whereas ROS, RNS, TNF- α , IL-1 β and IL-6 levels and eNOS and Nrf2 mRNA levels were significantly reduced. In conclusion, this study indicates that the ibuprofen-PEG/PLA -nanomicelles provide significant improvement in the motor function restoration and mitigation of inflammation and oxidative stress stimulated by SCI through eNOS/Nrf2 signaling pathway.

© 2021 The Author(s). Published by Elsevier B.V. on behalf of King Saud University. This is an open access article under the CC BY-NC-ND license (<http://creativecommons.org/licenses/by-nc-nd/4.0/>).

1. Introduction

Neurological disorders after spinal cord injuries (SCIs) occur as a result of primary mechanical damage and secondary degeneration process (Ahuja et al., 2017). The severity of these disorders depends on the extent of secondary damage caused by cellular, molecular, and biochemical events such as calcium ion infiltration into the cell, peroxidation due to free radicals, vascular and inflammatory reactions, and inflammatory reactions (Lu et al., 2000; Rouanet et al., 2017).

Studies have also shown that apoptosis is one of the most important and key mechanisms of secondary damage in SCIs due to numerous factors such as increased free radicals, cytokines and inflammatory responses (Zhang et al., 2012). However, in spinal cord lesions such as brain lesions, both necrotic and apoptotic cells are observed, so that as the lesion increases in severity; the number of necrotic cells also increases (Zhang et al., 2012).

In human SCIs and the animal experimental model, the spread of apoptosis (after weeks of lesion formation) is observed around the primary injured area (Beattie, 2004). After SCI, oligodendrocyte cells are highly susceptible to apoptosis and even exhibit receptors such as Fas and P75 that stimulate the onset of apoptosis (Casha et al., 2001).

Oligodendrocyte cell apoptosis causes demyelination of axons and neurological motor disorders (Casha et al., 2001). In recent years, research has focused on secondary spinal cord injuries (Oyinbo, 2011). Because the processes of this stage are somewhat preventable, including the use of anti-apoptotic compounds, free radical scavengers and anti-inflammatory agents (Oyinbo, 2011).

So far, various drug combinations have been used in the treatment of SCIs, including the use of corticosteroids, ganglioside, opioid antagonists, glutamate receptor antagonists and ion channels and cyclooxygenase inhibitors (Amar and Levy, 1999; Kwon et al., 2004; Karsy and Hawryluk, 2017; Venkatesh et al., 2019).

Indeed, using a substance that can reduce the severity of the lesions or intensify the healing process can solve many neurological disorders. Epidemiological studies have shown that long-term treatment with nonsteroidal anti-inflammatory drugs (NSAIDs), such as ibuprofen, reduces the risk of neurodegenerative diseases and delaying the onset of the disease, which confirms the role of inflammation in the onset and progression of SCI (Wang et al., 2009; Pires et al., 2017 Oct 1).

However, high-dose systemic ibuprofen may be used in the SCI could result in serious adverse effects which hamper neurological recovery (Cuzzolin et al., 2018). The unwanted effects of ibuprofen-based therapy are associated with the high systemic dosage and its cytotoxicity (Irvine et al., 2018). Therefore, development of some potential formulation of ibuprofen can improve its therapeutic and clinical application (Irvine et al., 2018).

The use of synthetic polymers in nerve tissue engineering has also received a great deal of interest due to their mechanical strength and flexibility with ease of modification and adaptability (Boni et al., 2018). Also, their structural properties can be modified through various methods, including combinations and addition of copolymers (Boni et al., 2018).

Polyethylene glycol (PEG) is a hydrophilic polymer with little ability to bind to cells. This compound has been shown to induce neuroprotective properties to reduce the oxidative stresses caused by SCI (Lu et al., 2018). Studies in SCI specimens have shown that the use of PEG inhibits apoptotic cell death following SCI and improves general motor function (Luo and Shi, 2007). Also, various homopolymers, copolymers and composites based on polylactic acid (PLA) have been prepared and used in various fields such as controlled drug delivery systems, orthopedic prostheses, bone fracture stabilizers, tooth restorations, tracheal replacement, hernia treatment, ligament renewal, and ligament renewal (DeStefano et al., 2020).

Therefore, a potential strategy can be developed to formulate ibuprofen by means of PEG to provide a synergic therapeutic effect against SCI.

Therefore, in the present study, PEG-poly lactide acid (PLA) diblock copolymer nanomicelles were developed as potential platforms for encapsulation of ibuprofen as well as promising therapeutic agents against SCI.

2. Materials and methods

2.1. Materials

Ibuprofen and PEG-block- PLA methyl ether, PEG average Mn 350, PLA average Mn 1000 diblock copolymer were obtained from Sigma-Aldrich Co. dissolved in 1% ethanol and diluted with phosphate buffered saline (PBS). All remaining materials were purchased from either Sigma-Aldrich Co. (St. Louis, MO, USA) or Merck Co. (Darmstadt, Germany).

2.2. Methods

2.2.1. Preparation of ibuprofen-PEG/PLA diblock copolymer nanomicelles

The PEG-PLA diblock copolymer (120 mg) and ibuprofen (10 mg) were hydrated in 15 mL of methanol, the sample was dried through reduced pressure at 37 °C and kept at vacuum for additional 8 h. The thin film was rehydrated in 4 mL of distilled water (DW) and filtrated through 0.22 µm Millipore filter.

2.3. Characterization of nanomicelle

The diameter of prepared nanomicelles were determined by transmission electron microscopy (TEM) analysis (JEM 2100F, Japan). The mean hydrodynamic radius and zeta potential of samples were also evaluated by dynamic light scattering (DLS) using a Zetasizer Nano ZS90 instrument (Malvern, UK).

2.4. Entrapment efficiency (EE) and drug loading (DL)

The loading amount of ibuprofen in PEG-PLA diblock copolymer nanomicelles was explored by LC-20AT HPLC system at 264 nm.

The percentage DL of ibuprofen-PEG/PLA diblock copolymer nanomicelles was analyzed through separating the untrapped cargo from nanomicelles by centrifugation (10,000 rpm, 15 min). Ibuprofen contents in the supernatant was then assessed through high-performance liquid chromatography (HPLC, LC-20AT, Shimadzu, Japan) at 264 nm equipped with Diamonsil 5 µm C18 column at 30 °C column temperature. The mobile phase was a mixture of acetonitrile and distilled water with a 60:40 vol ratio with a flow rate of 1.0 mL/min. The DL% and EE% were determined by the following equations (Li et al., 2018).

$$EE(\%) = \frac{\text{Weight of ibuprofen in nanomicelles}}{\text{Total weight of ibuprofen}} \times 100\%$$

$$DL(\%) = \frac{\text{Weight of ibuprofen in nanomicelles}}{\text{Weight of micelles containing}} \times 100\%$$

2.5. Serum stability of prepared nanomicelles

The ibuprofen-PEG/PLA diblock copolymer nanomicelles were stored at pH 7.4 PBS and 10% FBS for 120 h at 4 °C. The stability of the nanomicelles was then monitored by the alterations in particle size in the samples over time monitored by DLS.

2.6. Drug release kinetic

The *in vitro* release assay of ibuprofen from PEG-PLA diblock copolymer nanomicelles was assessed using dialysis method. In briefly, free ibuprofen (100 µg) or -ibuprofen-PEG/PLA diblock copolymer nanomicelles (with 100 µg ibuprofen) were poured into the dialysis bags (MWCO = 2500 Da, Rancho

Dominguez, CA) and placed in 20 mL of PBS (pH 7.4, 10% FBS) at 37 °C with stirring at 100 rpm for 120 h and at different time intervals, the samples were examined by HPLC method.

2.7. Animal handling

All experiments were carried out based on the animal ethics committees' guidelines approved at our University. Female Sprague-Dawley rats (220–250 g) were anesthetized using ketamine and xylazine and cervical laminectomy was done through the modified approach of SCI (Kim, 2016). Briefly, the muscles over the vertebral column C4–6 and the C5 spine segment were carefully removed, raised the cervical cord, severance was induced with surgical sharp blades #11.

The experimental groups ($n = 8$) were treated with PEG-PLA diblock copolymer, PEG-PLA diblock copolymer nanomicelle, ibuprofen, and ibuprofen-PEG/PLA diblock copolymer nanomicelles directly poured on the cervical cord and on the blades before severance for fast drug absorption. The group with SCI which received PBS was considered as the control group.

2.8. Electrophysiology assay

Five randomly rats per group were selected for electrophysiology assay 1 h after surgery. To examine electrophysiological function of the spinal motor, rats were fixed on a stereotaxic device and motor-evoked potentials (MEPs) were read employing a bipolar disk electrode in the sciatic nerve after stimulation (8 mA) of the hindlimb area based on the previous report (Kim, 2016).

2.9. Basso, Beattie and Bresnahan (BBB) locomotor rating scale

The motor function of the hind limbs was assessed by the BBB assay based on the standard BBB grading assessment. Scoring standards were as follows: 0–7, joint activity; 8–13, gait and coordination function; 14–21, claw movement.

2.10. Reactive oxygen species (ROS) assay

The level of ROS in spinal cord tissue (0.2 cm of the spinal cord) was explored using 2',7'-dichlorodihydrofluorescein diacetate (H₂DCF-DA) by spectrophotometer ($\lambda_{ex}/\lambda_{em}$: 495/523 nm). The cells were centrifuged at 1500 rpm for 10 min at 4 °C, followed by addition of H₂DCF-DA probe with a final concentration 10 µM, and incubation (30 min) in a dark. Finally, the DCF fluorescence was assessed.

2.11. Reactive nitrogen species (RNS) measurement

4-Amino-5-methylamino-2',7'-difluorofluorescein diacetate (DAF-FM Diacetate) was used to assess the level of RNS generation in investigated spinal cords by spectrophotometer ($\lambda_{ex}/\lambda_{em}$: 493/517 nm) as above described. The cells were incubated with the DAF-FM Diacetate (10 µM) for 30 min in a dark. Finally, the fluorescence intensity was measured.

Table 1 Primer sequences used for qPCR analysis.

Gene	Upstream primer sequence (5'-3')	Downstream primer sequence (5'-3')
eNOS	ACCGCCACACAGTAAATCCA	TGCCAACAGGAAGCTGAGAG
Nrf2	ATGAGTCGCTTGCCCTGG	CTTGTTTTCCGTATTAAG
β -actin	CTG TCCCTGTATGCCTCT	ATGTACGCACGATTCC

Abbreviation: eNOS, endothelial nitric oxide synthase; Nrf2, nuclear factor erythroid 2-related factor 2.

2.12. Elisa assay

Animals were killed after SCI by CO₂ inhalation and 0.2 cm of the spinal cord were sectioned, at the injured site. The level of cytokine and oxidative stress markers were then assessed by homogenation of the samples in PBS (pH 7.4), centrifuging (18,000 rpm, 30 min), and using the supernatant. The levels of TNF- α , IL-1 β , IL-6, superoxide dismutase (SOD), catalase (CAT), and glutathione (GSH) were then assessed with commercially available enzyme-linked immunosorbent assay (ELISA) (Biosource International, Camarillo, CA) kits and samples were run in duplicate.

2.13. Quantitative polymerase chain reaction (qPCR) analysis

The extraction of total RNA and synthesis of cDNA were carried out using commercially available kit (Thermo Fisher Scientific, Inc., USA) according to the manufacturer's instructions, in a real-time PCR system (RR820A; Takara Bio, Inc., Otsu, Japan). Primers (Table 1) were designed based on genes presented in GenBank.

The relative gene expression was assessed using the $2^{-\Delta\Delta C_t}$ assay.

2.14. Statistical analysis

Statistical analysis was performed using SPSS 25.0 software. The comparison between the two groups was performed by One-Way ANOVA. Paired *t*-test was used for comparison and Pearson correlation analysis was used for the correlation between the data, and *t* test was used for clinical efficacy. *P* < 0.05 was considered as statistically significant difference.

3. Results and discussion

3.1. Nanomicelle characterization

Diblock copolymer could self-assemble to form nanomicelles by filming-rehydration strategy. Under TEM, the morphology of ibuprofen-PEG/PLA diblock copolymer nanomicelles was illustrated in Fig. 1(A), showing mostly spheroidal shape with small size (Tong et al., 2011). The average diameter of ibuprofen-PEG/PLA diblock copolymer nanomicelles presented in Fig. 1A were analyzed to be in size range of 10–30 nm. Average hydrodynamic radius of blank PEG-PLA diblock copolymer nanomicelles was 32.4 ± 2.18 nm and ibuprofen-PEG/PLA diblock copolymer nanomicelles presented in Fig. 1B were found to be in size range of 36.2 ± 2.01 nm. The hydrodynamic radius of ibuprofen-PEG/PLA diblock copolymer nanomicelles was primarily consistent with that of free micelles, which indicated that the structure of PEG-PLA diblock copolymer nanomicelles was not disintegrated by encapsulating ibuprofen. Also, the hydrophobic forces among the nanomicelles moiety hold ibuprofen together to induce the formation of spherical nanomicelles with small geometry (Lu and Park, 2013). Moreover, the hydrodynamic radius of this nanomicelles was large enough to prevent being filtered out or metabolized by kidneys or liver, yet small enough to escape the macrophage engulfment (Wang et al., 2013). Therefore, the ibuprofen-PEG/PLA diblock copolymer nanomicelles with the particle size of 36.2 ± 2.01 nm could show slow metabolism and great stability and enough circulation time (Raza et al., 2016). Besides, zeta potential values of blank PEG-PLA diblock copolymer nanomicelles and ibuprofen-PEG/PLA diblock copolymer nanomicelles were

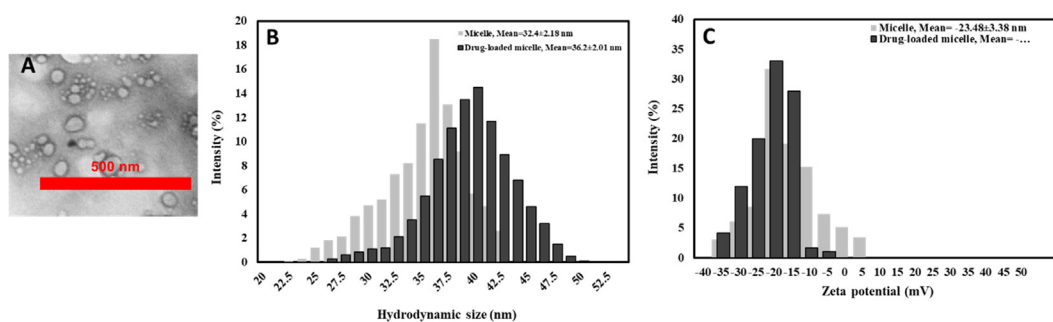


Fig. 1 Characterization of PEG/PLA diblock copolymer nanomicelles and ibuprofen-PEG/PLA diblock copolymer nanomicelles. (A) TEM image. (B) Size distribution. (C) Zeta potential.

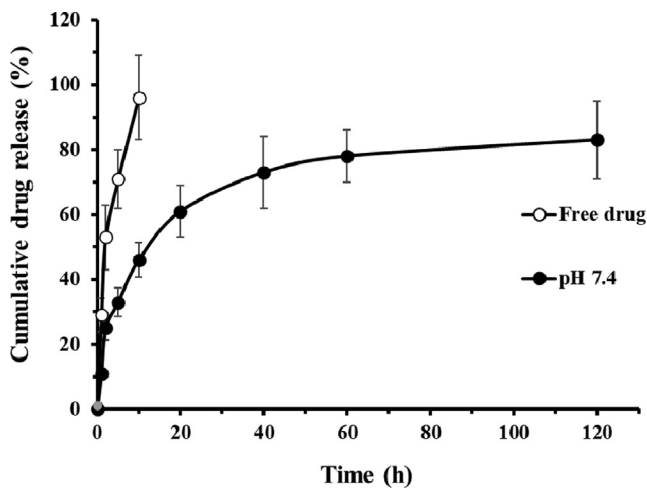


Fig. 2 *In vitro* study of ibuprofen-PEG/PLA diblock copolymer nanomicelles. Release profile of ibuprofen and ibuprofen-PEG/PLA diblock copolymer nanomicelles.

-21.73 ± 4.21 mV and -34.48 ± 3.38 M, respectively (Fig. 1C), indicating the potential loading of cargo and promising colloidal stability of fabricated nanomicells. Indeed, interparticle electrostatic interactions result in the colloidal stability of nanomicelles (Hu et al., 2014; Szilagy et al., 2014).

3.2. EE%, DL%, and *in vitro* stability

The DL% and EE% for ibuprofen-PEG/PLA diblock copolymer nanomicelles were around 9.3% and 72.09%, respectively. Ibuprofen-PEG/PLA diblock copolymer nanomicelles remained stable when stored at 4 °C for 120 h. Indeed, no nanomicelle hydrodynamic radius distribution changes were detected during 120 h. The high drug loading capacity and potential stability of ibuprofen-PEG/PLA diblock copolymer nanomicelles can be associated with the hydrophobic

interaction of the drugs and copolymers in solubilizing ibuprofen (Abouzeid et al., 2014). In consistent with previous reports, ibuprofen-PEG/PLA diblock copolymer nanomicelles incubation in the presence of 10% FBS 120 h demonstrated no difference in hydrodynamic radius or size distribution (Roby et al., 2006). Nanomicelles with potential colloidal stability over time can be promisingly stable in the blood over time (Dong et al., 2017).

3.3. *In vitro* drug release assay

As shown in Fig. 2, free ibuprofen was released rapidly, about 96% of the ibuprofen has been released during the first 10 h. In contrast, ibuprofen-PEG/PLA diblock copolymer nanomicelles revealed a slight burst release within the first 20 h, followed by a continuous release phase over 12 h. Only about 83% of ibuprofen was slowly released from ibuprofen-PEG/PLA diblock copolymer nanomicelles even after 120 h (Fig. 2). These data indicated that ibuprofen-PEG/PLA diblock copolymer nanomicelles provide relatively low leakage at physiological pH which can lead to a sustained high drug accumulation at the target site. Since the ibuprofen release is relatively slow, it suggests that the core of the ibuprofen-PEG/PLA diblock copolymer nanomicelles is stiff and glassy (Torchilin, 2005), which indicates less mobility to the encapsulated ibuprofen in comparison with the mobile cores (Gill et al., 2011 Oct 1). Therefore, the ibuprofen loaded into the inner core of PEG-PLA diblock copolymer nanomicelles was released in a sustained approach.

3.4. Electrophysiological assay

To analysis electrophysiological function of the spinal motor pathway, MEPs were read in the sciatic nerve upon stimulation (8 mA) of the hindlimb site of the sensorimotor cortex (Kim, 2016). MEP signal of sham -treated rats exhibited a

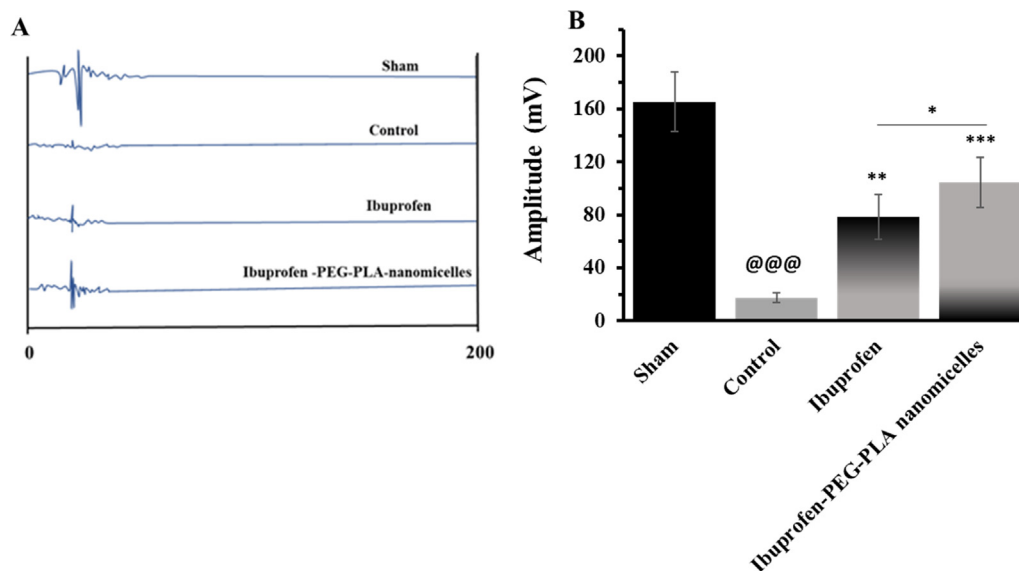


Fig. 3 Motor-evoked potential (MEP) analysis. (A) MEP graphs of different groups after surgery. (B) The average amplitude of different groups after surgery. Data represent the mean \pm S.D. of five rats in each group. @@@ $P < 0.001$, relative to sham-treated group, * $P < 0.05$, ** $P < 0.01$, *** $P < 0.001$, relative to control group.

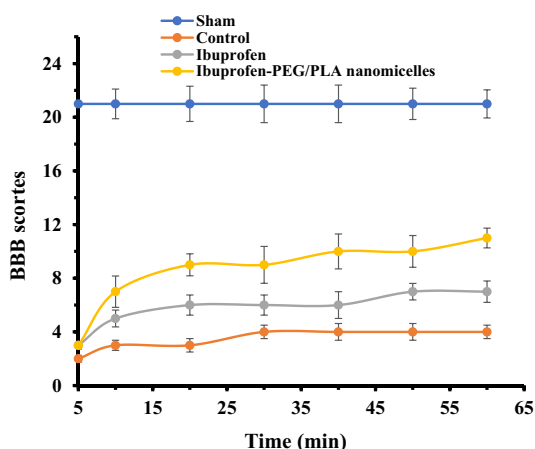


Fig. 4 BBB scores after SCI at different time intervals.

positive/negative deflection pattern (Fig. 3A), however did not display a similar pattern in all treated groups after surgery. However, as shown in Fig. 3B, it can be determined that the recorded amplitudes were relatively recovered in the case of ibuprofen and ibuprofen-PEG/PLA diblock copolymer nanomicelles. Fig. 3B shows the average MEP amplitudes recorded following SCI. In control group, MEP amplitude decreased to 17.41 ± 3.75 mV at 1 h after surgery, whereas MEP amplitudes in ibuprofen- and ibuprofen-PEG/PLA -treated animals were remarkably increased in comparison with the control group, and this enhancement was more pronounced for ibuprofen-PEG/PLA -treated animals (104.47 ± 18.76 mV; $P < 0.05$).

3.5. Hind limb motor function assay

As shown in Fig. 4, on time 5 min, none of the rats in the SCI and treated groups both with free ibuprofen of ibuprofen-PEG/PLA diblock copolymer nanomicelles scored higher than 3 points, suggesting that the spinal cord was completely injured and hind limb motor deactivation was significant. On time 10 min the motor function of the hind limbs in the treated

group was improved, with higher scores for ibuprofen-PEG/PLA diblock copolymer nanomicelles-treated group than those in the free ibuprofen treated-group.

3.6. Assessment of ROS and RNS levels

The molecular mechanisms behind the protective effects of the ibuprofen in the free or nano-formulated states was then assessed using fluorimetric assay exploring the generation of free radicals: ROS and RNS. The level of ROS (Fig. 5A) and RNS (Fig. 5B) generated by SCI was significantly higher than sham-treated group ($P < 0.001$). However, the obtained data indicated that the both free ibuprofen and ibuprofen-PEG/PLA diblock copolymer nanomicelles compounds can reduce the generation of ROS and RNS. Indeed, the marked reduction in the generation of ROS and RNS was more pronounced in the case of samples incubated with ibuprofen-PEG/PLA diblock copolymer nanomicelles than free ibuprofen.

3.7. Elisa assay

Compared with that in the control group, the levels of inflammatory cytokines including TNF- α (Fig. 6A), IL-1 β (Fig. 6B) and IL-6 (Fig. 6C) were significantly decreased, and the levels of SOD (Fig. 6D), CAT (Fig. 6E) and GSH (Fig. 6F) were significantly increased in the both free ibuprofen- and ibuprofen-PEG/PLA diblock copolymer nanomicelles-treated groups.

However, ibuprofen-PEG/PLA diblock copolymer nanomicelles significantly reduced the levels of inflammatory cytokines, and increased the levels of non-enzymatic and enzymatic antioxidant systems compared with that in the free ibuprofen group (Fig. 6).

3.8. qPCR assay

Compared with that in the sham group, the expression of eNOS (Fig. 7A) and Nrf2 (Fig. 7B) mRNA in spinal cord sample of the SCI group (control) was remarkably increased ($P < 0.001$). However, both free ibuprofen and

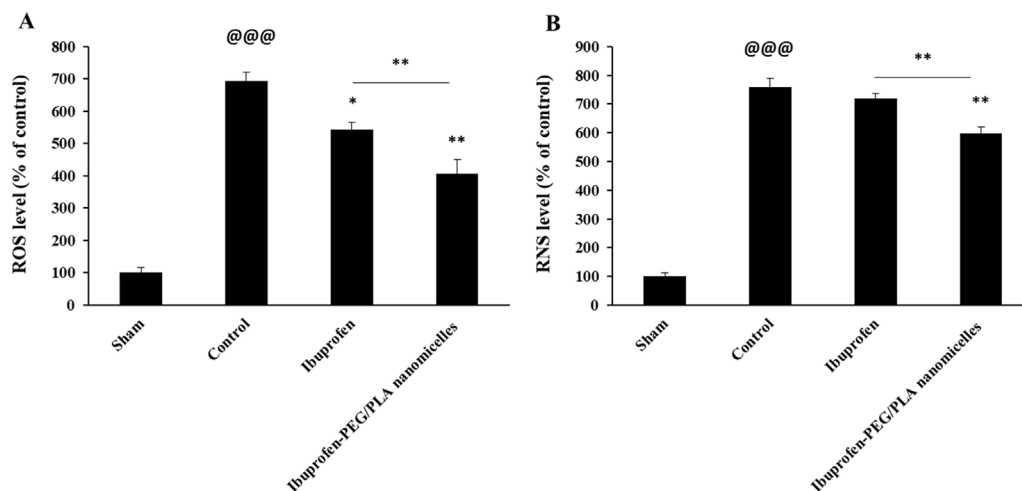


Fig. 5 SCI-induced changes in the spinal cord levels of ROS (A) and RNS (b) as determined by fluorimetric assay. Data represent the mean \pm S.D. of five rats in each group. @@@ $P < 0.001$, relative to sham-treated group, * $P < 0.05$, ** $P < 0.01$, relative to control group.

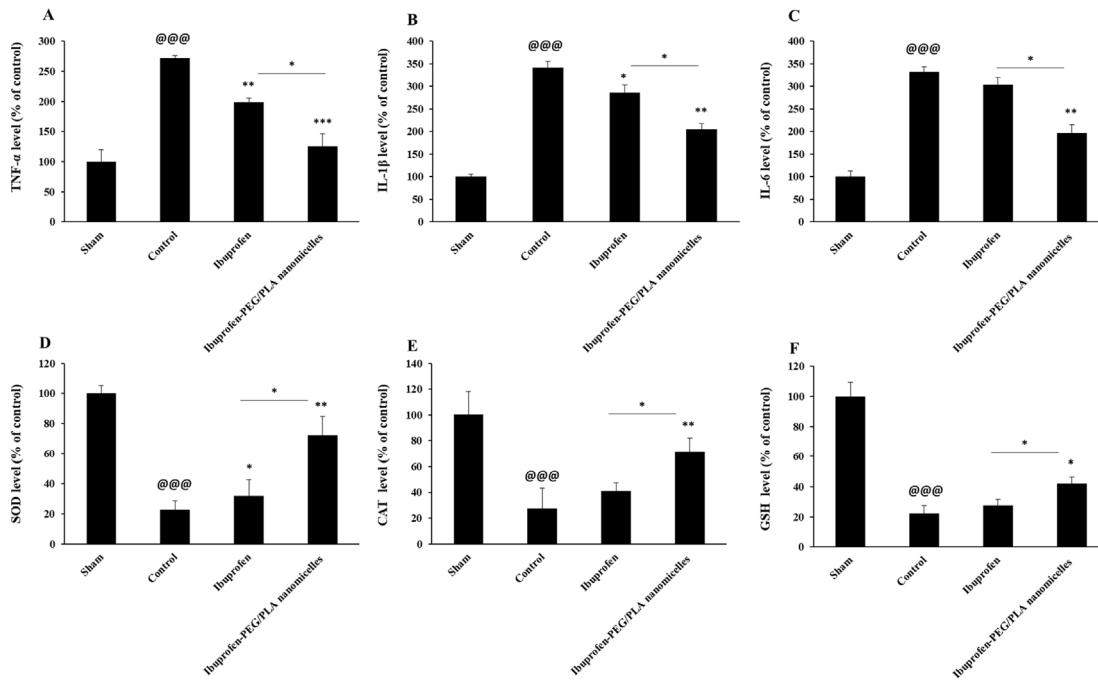


Fig. 6 SCI-stimulated changes in the spinal cord levels of TNF- α (A), IL-1 β (B), IL-6 (C), SOD (D), CAT (E), and GSH (F) as determined by ELISA. Data represent the mean \pm S.D. of five rats in each group. @@@ P < 0.001, relative to sham-treated group, * P < 0.05, ** P < 0.01, *** P < 0.001, relative to control group.

ibuprofen-PEG/PLA diblock copolymer nanomicelles significantly reduced eNOS and Nrf2 mRNA expression levels in comparison with that in the SCI group. Also, the decrement rate of ibuprofen-PEG/PLA diblock copolymer nanomicelles on the expression level of both mRNA was more pronounced than free drug.

4. Discussion

In the present study, the SCI has been affected cervically, as can be occurred due to head-body transference (Canavero,

2015). Being able to reconstruct cervical spinal cord motor function and mitigation of oxidative stress and inflammation may hold a great promise for treatment of SCI.

The balance between ROS/RNS production and removal in cells is maintained by several antioxidant mechanisms (Salim, 2017 Jan 1). Dysfunction of each of these mechanisms alters the oxidation–reduction state of the cell in favor of oxidative stress which produces the secondary injury after traumatic SCI (Patel, 2016 Sep 1). Cells by enzymes (SOD, CAT, glutathione peroxidase, glutathione reductase, and glutathione S-transferase) and intracellular antioxidant molecules (glutathione, selenium, vitamins) protect themselves against

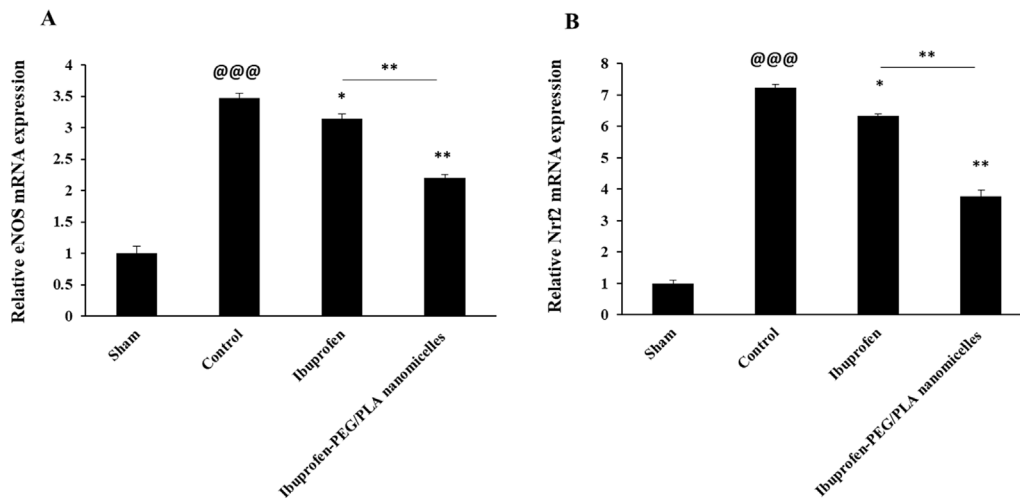


Fig. 7 SCI-stimulated changes in the spinal cord expression of eNOS mRNA (A) and Nrf2 mRNA (B) as determined by qPCR. Data represent the mean \pm S.D. of five rats in each group. @@@ P < 0.001, relative to sham-treated group, * P < 0.05, ** P < 0.01, relative to control group.

oxidative stress (Kabel, 2014). However, sometimes external stimuli and intracellular metabolic changes lead to increased ROS/RNS or decreased antioxidant capacity and impaired redox homeostasis, resulting in exposure to large amounts of ROS/RNS that cannot be detoxified by intracellular antioxidants which needs development of antioxidant therapies (Villa et al., 2019 Apr). Under these conditions, ROS/RNS irreversibly enter the structure of macromolecules and alter cell functions (Ahmad et al., 2017 Dec).

ROS and RNS are involved in several cascades of cell injury, such as cell death, angiogenesis, differentiation, and inflammation (Ryter et al., 2007 Jan 1). ROS and RNS usually cause reversible oxidation of target proteins such as tyrosine phosphatases, tyrosine kinases, and some transcription factors such as NF- κ B, Nrf2, AP-1, and 1α -HIF (Morel and Barouki, 1999 Sep 15; Pendyala and Natarajan, 2010 Dec 31; KumaráSharma, 2015).

Nitric oxide synthase isoforms (nNOS, iNOS, eNOS) are expressed in the central nervous system (CNS) and play several key roles, including intracellular messaging and neurotransmission (Yilmaz et al., 2020 Sep). In the CNS, eNOS expression is not significant unless cellular stimulation occurs, and after stimulation, eNOS is overexpressed by a variety of cells, such as macrophages, microglia, astrocytes, oligodendrocytes, and even endothelial cells (Pechanova et al., 2020 Dec; Xu et al., 2020 May 15). Numerous studies have shown that NO may be involved in the pathogenesis of various neuroinflammatory/neurodegenerative diseases (Pechanova et al., 2020 Dec; Caviedes et al., 2021 Jan 4).

eNOS expression is usually associated with inflammatory conditions and is abundantly produced by a variety of monocyte-macrophage cells (Ariff et al., 2020 Dec). NO derived from eNOS is released locally from inflammatory cells in response to inflammatory stimuli of the CNS (Choi et al., 2019 Feb; Liu et al., 2018 Aug 1).

Excessive levels of NO in the SC are associated with tissue damage due to SCI (Gao and Li, 2017 Dec). Because NO is produced in both central and peripheral nerves, a drug like ibuprofen that suppresses the production of NO products by inhibiting eNOS can be used as a promising treatment for some types of SCI. The balance between the positive and negative effects of eNOS-derived NO in the SCI is complex and must be carefully weighed. For example, it has been reported that ibuprofen promotes recovery from SCI by inhibiting tissue loss (Wang et al., 2009 Jan 1), inducing axonal elongation (Wang et al., 2009 Jan 1; Sharp et al., 2013 Oct), and reducing C-reactive protein and interleukin-6 levels (Park et al., 2020 Jun). However, there are some reports which indicated that ibuprofen could not lead to neuroprotection (Redondo-Castro and Navarro, 2014 Feb) or enhanced histologic or functional outcome (Streijger et al., 2014 Jul) after SCI.

Therefore, the nano-formulation of drugs has been shown to improve their stability, bioavailability, pharmacokinetic and pharmacodynamic properties (Gigliobianco et al., 2018 Sep; Bhakay et al., 2018 Sep; Khan et al., 2020 Apr). Also, it has been reported that methylprednisolone loaded ibuprofen modified dextran nanoparticles can be applied for drug delivery in acute SCI (Qi et al., 2017 Nov 21). In agreement with some other reports, we also showed that PEG/PLA diblock copolymer nanomicelles can increase the bioavailability, stability, and protective effects of ibuprofen.

Although these data are basic outcomes that require to be approved by more detailed investigations, it seems that immediately recovering the MEP amplitude can result in a process resulting in neurophysiological recovery.

5. Conclusion

Although more detailed research in this field is necessary to potentially explore the mechanisms of ibuprofen in the reconstruction of the cervical spinal cord and motor function recovery, the data of the present study suggest that the application of ibuprofen-PEG/PLA diblock copolymer nanomicelles may be useful in rapid recovery of motor function and reduction of oxidative stress and expression of inflammatory cytokines after SCI. The precise role of motor function in the treatment of SCI and neuroprotection remains to be determined.

6. Consent for publication

All authors agreed and approved the consent for publication

Ethical statement

All animal use procedures were carried out in accordance with the Regulations of Experimental Animal Administration issued by the State Committee of Science and Technology of the People's Republic of China, with the approval of the Ethics Committee in our university.

CRediT authorship contribution statement

Yang Yang: Methodology, Analysis, Verification, Revision.
Lei Zhang: Methodology, Analysis, Verification, Revision.
Meiyi Huang: Methodology, Analysis, Verification, Revision.
Rubo Sui: Conceptualization, Supervision.
Suliman Khan: Conceptualization, Supervision, Writing the manuscript.

Declaration of Competing Interest

The authors declare that they have no known competing financial interests or personal relationships that could have appeared to influence the work reported in this paper.

Acknowledgements

The authors gratefully acknowledge the China Postdoctoral Science Foundation research grant No. 2020M672291.

References

- Ahuja, C.S., Schroeder, G.D., Vaccaro, A.R., Fehlings, M.G., 2017. Spinal cord injury—what are the controversies?. *J. Orthop. Trauma* 31, S7–S13.
- Lu, J., Ashwell, K.W., Waite, P., 2000. Advances in secondary spinal cord injury: role of apoptosis. *Spine* 25 (14), 1859–1866.
- Rouanet, C., Reges, D., Rocha, E., Gagliardi, V., Silva, G.S., 2017. Traumatic spinal cord injury: current concepts and treatment update. *Arq. Neuropsiquiatr.* 75 (6), 387–393.
- Zhang, N., Yin, Y., Xu, S.J., Wu, Y.P., Chen, W.S., 2012. Inflammation & apoptosis in spinal cord injury. *Ind. J. Med. Res.* 135 (3), 287.

- Beattie, M.S., 2004. Inflammation and apoptosis: linked therapeutic targets in spinal cord injury. *Trends Mol. Med.* 10 (12), 580–583.
- Casha, S., Yu, W.R., Fehlings, M.G., 2001. Oligodendroglial apoptosis occurs along degenerating axons and is associated with FAS and p75 expression following spinal cord injury in the rat. *Neuroscience* 103 (1), 203–218.
- Oyinbo, C.A., 2011. Secondary injury mechanisms in traumatic spinal cord injury: a nugget of this multiply cascade. *Acta Neurobiol. Exp. (Wars)* 71 (2), 281–299.
- Amar, A.P., Levy, M.L., 1999. Pathogenesis and pharmacological strategies for mitigating secondary damage in acute spinal cord injury. *Neurosurgery* 44 (5), 1027–1039.
- Kwon, B.K., Tetzlaff, W., Grauer, J.N., Beiner, J., Vaccaro, A.R., 2004. Pathophysiology and pharmacologic treatment of acute spinal cord injury. *Spine J.* 4 (4), 451–464.
- Karsy, M., Hawryluk, G., 2017. Pharmacologic management of acute spinal cord injury. *Neurosurg. Clin.* 28 (1), 49–62.
- Venkatesh, K., Ghosh, S.K., Mullick, M., Manivasagam, G., Sen, D., 2019. Spinal cord injury: pathophysiology, treatment strategies, associated challenges, and future implications. *Cell Tissue Res.* 1–27.
- Wang, X., Budel, S., Baughman, K., Gould, G., Song, K.H., Strittmatter, S.M., 2009. Ibuprofen enhances recovery from spinal cord injury by limiting tissue loss and stimulating axonal growth. *J. Neurotrauma* 26 (1), 81–95.
- Pires, L.R., Lopes, C.D., Salvador, D., Rocha, D.N., Pêgo, A.P., 2017 Oct 1. Ibuprofen-loaded fibrous patches—taming inhibition at the spinal cord injury site. *J. Mater. Sci. - Mater. Med.* 28 (10), 157.
- Cuzzolin, L., Bardanzellu, F., Fanos, V., 2018. The dark side of ibuprofen in the treatment of patent ductus arteriosus: could paracetamol be the solution?. *Expert Opin. Drug Metab. Toxicol.* 14 (8), 855–868.
- Irvine, J., Afrose, A., Islam, N., 2018. Formulation and delivery strategies of ibuprofen: challenges and opportunities. *Drug Dev. Ind. Pharm.* 44 (2), 173–183.
- Boni, R., Ali, A., Shavandi, A., Clarkson, A.N., 2018. Current and novel polymeric biomaterials for neural tissue engineering. *J. Biomed. Sci.* 25 (1), 90.
- Lu, X., Perera, T.H., Aria, A.B., Callahan, L.A.S., 2018. Polyethylene glycol in spinal cord injury repair: a critical review. *J. Experim. Pharmacol.* 10, 37.
- Luo, J., Shi, R., 2007. Polyethylene glycol inhibits apoptotic cell death following traumatic spinal cord injury. *Brain Res.* 1155, 10–16.
- DeStefano, V., Khan, S., Tabada, A., 2020. Applications of PLA in modern medicine. *Eng. Regen.* 1, 76–87.
- Li, W., Wu, J., Zhang, J., Wang, J., Xiang, D., Luo, S., Li, J., Liu, X., 2018. Puerarin-loaded PEG-PE micelles with enhanced anti-apoptotic effect and better pharmacokinetic profile. *Drug Deliv.* 25 (1), 827–837.
- Kim, C.Y., 2016. PEG-assisted reconstruction of the cervical spinal cord in rats: Effects on motor conduction at 1 h. *Spinal cord* 54 (10), 910–912.
- Tong, S., Hou, S., Ren, B., Zheng, Z., Bao, G., 2011. Self-assembly of phospholipid-PEG coating on nanoparticles through dual solvent exchange. *Nano Lett.* 11 (9), 3720–3726.
- Lu, Y., Park, K., 2013. Polymeric micelles and alternative nanonized delivery vehicles for poorly soluble drugs. *Int. J. Pharm.* 453 (1), 198–214.
- Wang, B., He, X., Zhang, Z., Zhao, Y., Feng, W., 2013. Metabolism of nanomaterials in vivo: blood circulation and organ clearance. *Acc. Chem. Res.* 46 (3), 761–769.
- Raza, K., Kumar, N., Misra, C., Kaushik, L., Guru, S.K., Kumar, P., Malik, R., Bhushan, S., Katare, O.P., 2016. Dextran-PLGA-loaded docetaxel micelles with enhanced cytotoxicity and better pharmacokinetic profile. *Int. J. Biol. Macromol.* 88, 206–212.
- Hu, X., Yang, F.F., Quan, L.H., Liu, C.Y., Liu, X.M., Ehrhardt, C., Liao, Y.H., 2014. Pulmonary delivered polymeric micelles—pharmacokinetic evaluation and biodistribution studies. *Eur. J. Pharm. Biopharm.* 88 (3), 1064–1075.
- Szilagyi, I., Trefalt, G., Tiraferri, A., Maroni, P., Borkovec, M., 2014. Polyelectrolyte adsorption, interparticle forces, and colloidal aggregation. *Soft Matter* 10 (15), 2479–2502.
- Abouzeid, A.H., Patel, N.R., Torchilin, V.P., 2014. Polyethylene glycol-phosphatidylethanolamine (PEG-PE)/vitamin E micelles for co-delivery of paclitaxel and curcumin to overcome multi-drug resistance in ovarian cancer. *Int. J. Pharm.* 464 (1–2), 178–184.
- Roby, A., Erdogan, S., Torchilin, V.P., 2006. Solubilization of poorly soluble PDT agent, meso-tetraphenylporphyrin, in plain or immunotargeted PEG-PE micelles results in dramatically improved cancer cell killing in vitro. *Eur. J. Pharm. Biopharm.* 62 (3), 235–240.
- Dong, Z., Guo, J., Xing, X., Zhang, X., Du, Y., Lu, Q., 2017. RGD modified and PEGylated lipid nanoparticles loaded with puerarin: formulation, characterization and protective effects on acute myocardial ischemia model. *Biomed. Pharmacother.* 89, 297–304.
- Torchilin, V.P., 2005. Lipid-core micelles for targeted drug delivery. *Curr. Drug Deliv.* 2 (4), 319–327.
- Gill, K.K., Nazzal, S., Kaddoumi, A., 2011 Oct 1. Paclitaxel loaded PEG5000–DSPE micelles as pulmonary delivery platform: formulation characterization, tissue distribution, plasma pharmacokinetics, and toxicological evaluation. *Eur. J. Pharm. Biopharm.* 79 (2), 276–284.
- Canavero, S., 2015. The “Gemini” spinal cord fusion protocol: Reloaded. *Surg. Neurol. Int.* 6, 1–10.
- Salim, S., 2017 Jan 1. Oxidative stress and the central nervous system. *J. Pharmacol. Exp. Ther.* 360 (1), 201–205.
- Patel, M., 2016 Sep 1. Targeting oxidative stress in central nervous system disorders. *Trends Pharmacol. Sci.* 37 (9), 768–778.
- Kabel, A.M., 2014. Free radicals and antioxidants: role of enzymes and nutrition. *World J. Nutrit. Health.* 2 (3), 35–38.
- Villa, J.V., Villamar, D.M., Zapien, J.A., Espinoza, L.B., García, J.H., García, R.S., 2019 Apr. Current developments in antioxidant therapies for spinal cord injury. *Spinal Cord Injury Therapy.* 10, 1–32.
- Ahmad, W., Ijaz, B., Shabbiri, K., Ahmed, F., Rehman, S., 2017 Dec. Oxidative toxicity in diabetes and Alzheimer’s disease: mechanisms behind ROS/RNS generation. *J. Biomed. Sci.* 24 (1), 1.
- Ryter, S.W., Kim, H.P., Hoetzel, A., Park, J.W., Nakahira, K., Wang, X., Choi, A.M., 2007 Jan 1. Mechanisms of cell death in oxidative stress. *Antioxid. Redox Sign.* 9 (1), 49–89.
- Morel, Y., Barouki, R., 1999 Sep 15. Repression of gene expression by oxidative stress. *Biochem. J.* 342 (3), 481–496.
- Pendyala, S., Natarajan, V., 2010 Dec 31. Redox regulation of Nox proteins. *Respir. Physiol. Neurobiol.* 174 (3), 265–271.
- KumaráSharma, A., 2015. Reactive oxygen species: friend or foe?. *RSC Adv.* 5 (71), 57267–57276.
- Yilmaz, O., Soygüder, Z., Keleş, Ö.F., Yaman, T., Yener, Z., Uyar, A., Çakır, T., 2020 Sep. An immunohistochemical study on the presence of nitric oxide synthase isoforms (nNOS, iNOS, eNOS) in the spinal cord and nodose ganglion of rats receiving ionising gamma radiation to their liver. *J. Veterin. Res.* 64 (3), 445.
- Pechanova, O., Vrankova, S., Cebova, M., 2020 Dec. Chronic L-Name-Treatment Produces Hypertension by Different Mechanisms in Peripheral Tissues and Brain: Role of Central eNOS. *Pathophysiology.* 27 (1), 46–54.
- Xu, M.M., Seyler, L., Bäuerle, T., Kalinichenko, L.S., Müller, C.P., Huttner, H.B., Schwab, S., Manaenko, A., 2020 May 15. Serelaxin activates eNOS, suppresses inflammation, attenuates developmental delay and improves cognitive functions of neonatal rats after germinal matrix hemorrhage. *Sci. Rep.* 10 (1), 1. 1.
- Caviedes, A., Maturana, B., Corvalán, K., Engler, A., Gordillo, F., Varas-Godoy, M., Smalla, K.H., Batiz, L.F., Lafourcade, C., Kaehne, T., Wyneken, U., 2021 Jan 4. eNOS-dependent S-nitrosylation of the NF- κ B subunit p65 has neuroprotective effects. *Cell Death Dis.* 12 (1), 1–4.

- Ariff, A.M., Bakar, N.A., Muid, S.A., Omar, E., Ismail, N.H., Ali, A. M., Kasim, N.A., Nawawi, H.M., 2020 Dec. Ficus deltoidea suppresses endothelial activation, inflammation, monocytes adhesion and oxidative stress via NF- κ B and eNOS pathways in stimulated human coronary artery endothelial cells. *BMC Complem. Med. Therap.* 20 (1), 1–3.
- Choi, S., Saxena, N., Dhammu, T., Khan, M., Singh, A.K., Singh, I., Won, J., 2019 Feb. Regulation of endothelial barrier integrity by redox-dependent nitric oxide signaling: implication in traumatic and inflammatory brain injuries. *Nitric Oxide* 1 (83), 51–64.
- Liu, X., Gu, X., Yu, M., Zi, Y., Yu, H., Wang, Y., Xie, Y., Xiang, L., 2018 Aug 1. Effects of ginsenoside Rb1 on oxidative stress injury in rat spinal cords by regulating the eNOS/Nrf2/HO 1 signaling pathway. *Experim. Therap. Med.* 16 (2), 1079–1086.
- Gao, W., Li, J., 2017 Dec. Targeted siRNA delivery reduces nitric oxide mediated cell death after spinal cord injury. *J. Nanobiotechnol.* 15 (1), 1. 1.
- Wang, X., Budel, S., Baughman, K., Gould, G., Song, K.H., Strittmatter, S.M., 2009 Jan 1. Ibuprofen enhances recovery from spinal cord injury by limiting tissue loss and stimulating axonal growth. *J. Neurotrauma* 26 (1), 81–95.
- Sharp, K.G., Yee, K.M., Stiles, T.L., Aguilar, R.M., Steward, O., 2013 Oct. A re-assessment of the effects of treatment with a non-steroidal anti-inflammatory (ibuprofen) on promoting axon regeneration via RhoA inhibition after spinal cord injury. *Exp. Neurol.* 1 (248), 321–337.
- Park, A., Anderson, D., Battaglino, R.A., Nguyen, N., Morse, L.R., 2020 Jun. Ibuprofen use is associated with reduced C-reactive protein and interleukin-6 levels in chronic spinal cord injury. *J. Spinal Cord Med.* 5, 1–9.
- Redondo-Castro, E., Navarro, X., 2014 Feb. Chronic ibuprofen administration reduces neuropathic pain but does not exert neuroprotection after spinal cord injury in adult rats. *Exp. Neurol.* 1 (252), 95–103.
- Streijger, F., Lee, J.H., Duncan, G.J., Ng, M.T., Assinck, P., Bhatnagar, T., Plunet, W.T., Tetzlaff, W., Kwon, B.K., 2014 Jul. Combinatorial treatment of acute spinal cord injury with ghrelin, ibuprofen, C16, and ketogenic diet does not result in improved histologic or functional outcome. *J. Neurosci. Res.* 92 (7), 870–883.
- Gigliobianco, M.R., Casadidio, C., Censi, R., Di Martino, P., 2018 Sep. Nanocrystals of poorly soluble drugs: drug bioavailability and physicochemical stability. *Pharmaceutics.* 10 (3), 134.
- Bhakay, A., Rahman, M., Dave, R.N., Bilgili, E., 2018 Sep. Bioavailability enhancement of poorly water-soluble drugs via nanocomposites: Formulation-Processing aspects and challenges. *Pharmaceutics.* 10 (3), 86.
- Khan, T.I., Hemalatha, S., Waseem, M., 2020 Apr. Promising role of nano-encapsulated drugs for spinal cord injury. *Mol. Neurobiol.* 57 (4), 1978–1985.
- Qi, L., Jiang, H., Cui, X., Liang, G., Gao, M., Huang, Z., Xi, Q., 2017 Nov 21. Synthesis of methylprednisolone loaded ibuprofen modified dextran based nanoparticles and their application for drug delivery in acute spinal cord injury. *Oncotarget.* 8 (59), 99666.